

Structural Elucidation of Phototransformation Products of Azimsulfuron in Water

M. VITTORIA PINNA,[†] MICHELE ZEMA,[§] CARLO GESSA,[‡] AND ALBA PUSINO^{*,†}

Dipartimento di Scienze Ambientali Agrarie e Biotecnologie Agro-Alimentari, Università di Sassari, Viale Italia 39, 07100 Sassari, Italy; Dipartimento di Scienze della Terra, Università di Pavia, Via Ferrata 1, 27100 Pavia, Italy; and Dipartimento di Scienze Tecnologie Agro-Ambientali, Università di Bologna, Viale Fanin 40, 40127 Bologna, Italy

The photodegradation of the sulfonylurea herbicide azimsulfuron, *N*-[[[4,6-dimethoxypyrimidin-2-yl)-amino]carbonyl]-1-methyl-4-(2-methyl-2*H*-tetrazole-5-yl)-1*H*-pyrazole-5-sulfonamide (AZS), was studied in water at different wavelengths and in the presence of photocatalysts. AZS was rapidly degraded by UV light, affording three photoproducts. The main product, accounting for about 70% of photodegraded herbicide, was identified as 6-amino-5-[[[4,6-dimethoxypyrimidin-2-yl)methylamino]-1,5,6,8-tetrahydro-7-oxa-8λ⁶-tia-1,2,5,6-tetraza-azulen-4-one (ADTA) by single-crystal X-ray diffraction. With simulated sunlight irradiation, the reaction was slower and 2-amino-4,6-dimethoxypyrimidine (DPA) and 1-methyl-4-(2-methyl-2*H*-tetrazole-5-yl)-1*H*-pyrazole-5-sulfonamide (MPS), arising from a photohydrolytic cleavage of the sulfonylurea bridge, were the only byproducts observed. The reactions followed first-order kinetics. The addition of dissolved organic matter (DOM) did not modify significantly the AZS photodegradation rate. The presence of Fe₂O₃ accelerated more than twice the reaction rate affording two major products, DPA and MPS, together with minor amounts of *N*-[[[5-hydroxy-4,6-dimethoxypyrimidin-2-yl)amino]carbonyl]-1-methyl-4-(2-methyl-2*H*-tetrazole-5-yl)-1*H*-pyrazole-5-sulfonamide (AZS-OH). The greatest degradation rate was detected in the presence of TiO₂. Only the photohydroxylation product AZS-OH was observed, which was transformed rapidly into oxalic acid.

KEYWORDS: Azimsulfuron; photocatalysis; iron oxide; titanium oxide; DOM

INTRODUCTION

Azimsulfuron (AZS, trade name Gulliver, **Figure 1**) is a sulfonylurea herbicide used for the postemergence control of *Echinochloa* species, broadleaf, and sedge weeds in rice production. Like other sulfonylureas, it inhibits the activity of acetolactate synthase (ALS), which is essential in the biosynthesis of the branched-chain amino acids valine, leucine, and isoleucine (*1*).

Several studies have shown that AZS has favorable toxicological and environmental fate characteristics. The most significant degradation mechanisms for AZS in rice paddies are microbial metabolism in soil and indirect photolysis (*2*).

The degradation due to sunlight is important for the dissipation of pesticides in rice paddies. Clear and shallow water filters a very small amount of the incident light and allows both direct and indirect photochemical processes to occur in water and at the sediment–water interface. On the other hand, sulfonylurea herbicides are susceptible to direct (*3–5*) and indirect photolysis

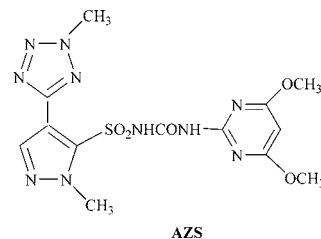


Figure 1. Chemical structure of AZS.

(*6, 7*). The major photoproducts arise from the cleavage of the sulfonylurea bridge, but further conversion products can be formed by dechlorination, hydrolysis, and cyclization. According to a European Community (EC) directive (*8*), the phototransformation of pesticides having a molar extinction coefficient (ϵ) of $>10 \text{ L mol}^{-1} \text{ cm}^{-1}$ for $\lambda \geq 290 \text{ nm}$ must be taken in account.

At $\lambda = 290 \text{ nm}$ AZS shows an ϵ value of $156 \text{ L mol}^{-1} \text{ cm}^{-1}$. No studies concerning the phototransformation products of AZS are available. Therefore, we studied the photochemical behavior of AZS in water at different wavelengths. Furthermore, the sunlight indirect photolysis was investigated in the presence of dissolved organic matter (DOM) and iron(III) oxide, two photocatalysts naturally present in paddy fields, and titanium

* Author to whom correspondence should be addressed (telephone +39 79 229219; fax +39 79 229276; e-mail pusino@uniss.it).

[†] Università di Sassari.

[§] Università di Pavia.

[‡] Università di Bologna.

Table 1. AZS Physical and Chemical Properties

melting point	170 °C
vapor pressure	4×10^{-9} Pa (25 °C)
solubility in water (mg L ⁻¹ , 20 °C)	72.3 (pH 5); 1050 (pH 7); 6536 (pH 9)
solubility in organic solvents (g L ⁻¹ , 25 °C)	acetone, 26.4; methanol, 2.1; hexane, <0.2; acetonitrile, 13.9; methylene chloride, 65.9; ethyl acetate, 13.0; toluene, 1.8
partition coefficient (log P_{ow} , 25 °C)	4.43 (pH 5); 0.043 (pH 7); 0.008 (pH 9)
dissociation constant	$pK_a = 3.6$
surface tension	68.1×10^{-3} Nm (23.7 °C)

dioxide. The major products were identified, and degradation pathways are proposed.

MATERIALS AND METHODS

Materials. AZS (99.7% purity) was supplied by DuPont de Nemours France SA (Centre Europeen de Recherches), Nambshheim, France. Some chemical and physical properties of AZS are reported in **Table 1**.

Its purity was checked by high-performance chromatography (HPLC). The photoproducts 2-amino-4,6-dimethoxypyrimidine (DPA, 98.0% purity, **Scheme 1**) and acetic, malonic, and oxalic acids were supplied by Aldrich, Milano, Italy. All of the solvents were of HPLC grade (Carlo Erba Reagenti, Milano, Italy) and were used without further purification.

DOM was obtained from a sediment collected in a paddy field near Novara (Italy). The sediment was air-dried and sieved to <2 mm. DOM was extracted by shaking overnight a 1 kg sample of the sediment (<2 mm fraction) with 2 L of distilled water. Then the suspension was filtered through a Durapore membrane filter 0.45 μ m (Millipore), and the filtrate was freeze-dried. Approximately 200 mg of DOM was obtained from 1 kg of sediment.

Hydrated ferric oxide was prepared by the addition of 500 mL of 1 N FeCl₂ to 250 mL of 2 M KOH under rapid stirring (9). The fresh precipitate was immediately washed with distilled water and dried under vacuum. X-ray analysis showed it to be amorphous. In addition, it was completely soluble in ammonium oxalate (pH 3).

Titanium dioxide (TiO₂, purity = 99.9%, density = 3.9 g mL⁻¹), predominantly anatase, was supplied by Aldrich, Milano, Italy.

Photolysis. The UV spectrum of AZS exhibits an intense absorption at 240 nm and a weaker band at 288 nm (**Figure 2**).

Direct photolysis experiments were carried out by irradiating 100 mL of an AZS aqueous solution (8 μ M). For 254 nm experiments, the device consisted of four low-pressure mercury lamps (RPR-2537 Å) mounted in a circle in a merry-go-round Rayonet photoreactor (5). The AZS solution, in a water-cooled quartz flask, was irradiated with an average irradiation intensity of 110 mW/cm².

Four black light fluorescent lamps (RPR-3500 Å) emitting in the range 250–600 nm, with a maximum emission at 366 nm and an average irradiation intensity of 175 mW/cm², were used to simulate sunlight irradiation. A water-cooled borosilicate flask, cutting the radiation shorter than 290 nm to simulate a part of the solar radiation, was the reaction vessel.

On the basis of preliminary trials, indirect photolysis experiments were carried out by adding 5 mg samples of colloid (TiO₂, Fe₂O₃, DOM) to 100 mL of an AZS aqueous solution (10 μ M). The suspension was stirred in the dark until equilibrium was reached, that is, the AZS concentration in the suspension became constant. After equilibration was achieved (1 and 1.5 h for TiO₂ and Fe₂O₃, respectively), the suspensions were irradiated in a merry-go-round Rayonet photoreactor with four black light fluorescent lamps. The suspension homogeneity and the exchange with the gaseous phase (air) were ensured by magnetic stirring. To trap hydroxyl radicals, further photocatalytic experiments were carried out by adding traces of isopropanol, an OH[•] scavenger, to the photolysis mixture. In this case, after the equilibration time, 10 μ L of the alcohol was added to suspensions containing TiO₂ or Fe₂O₃,

respectively, and the suspensions were then irradiated as described above. At regular intervals, AZS aqueous suspensions (0.5 mL) were collected and filtered through a 0.2 μ m filter (Whatman) to remove colloid particles. The filtrates were analyzed by HPLC.

Dark control experiments were carried out in conditions similar to those described above, except that the photoreaction vessel was covered by aluminum foil.

To study the kinetics of photodegradation, at appropriate times, depending on the photolysis rate, each test solution was analyzed directly by HPLC. All of the experiments were run in triplicate, and the kinetic data reported under Results and Discussion are the average values derived as the mean of three trials.

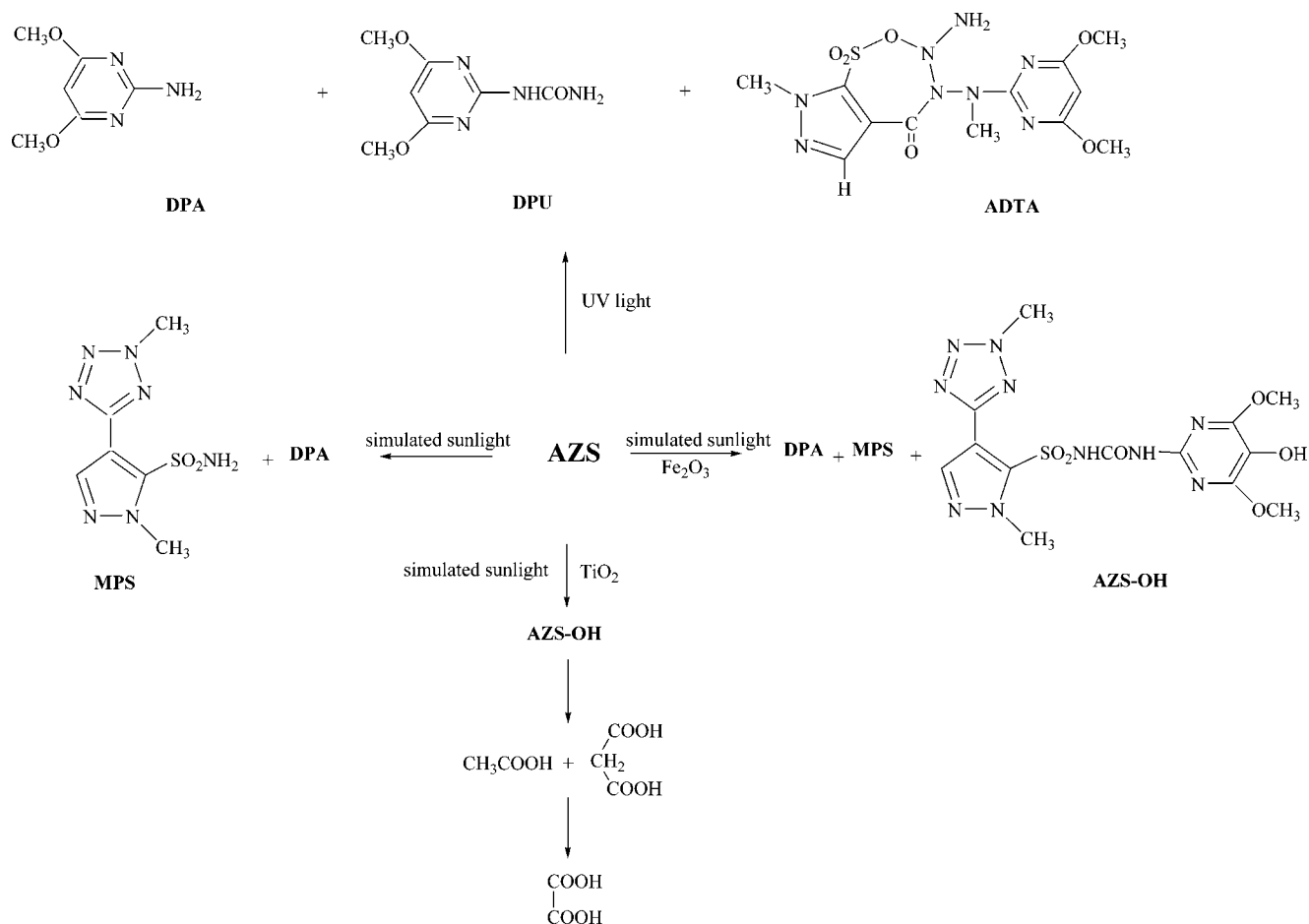
HPLC Analysis. AZS and its photodegradation products were estimated by HPLC. For direct photolysis a Waters 1515 liquid chromatograph equipped with a 250 \times 4 mm i.d. Bondapak C₁₈ (10 μ m) analytical column, a multiwavelength Waters 2487 UV-vis programmable detector operating at 240 nm, and a Breeze chromatography workstation were used. Acetonitrile plus water (50 + 50 by volume), previously brought to pH 2.7 with phosphoric acid, at a flow rate of 0.5 mL min⁻¹, was the eluant. The retention times were 9.8, 8.0, 6.9, 5.9, and 7.4 min for AZS, ADTA, DPA, DPU, and 1-methyl-4-(2-methyl-2H-tetrazole-5-yl)-1H-pyrazole-5-sulfonamide (MPS), respectively (**Scheme 1**).

For indirect photolysis a Waters 1515 liquid chromatograph equipped with a 300 \times 3.9 mm i.d. Bondapak C₁₈ (10 μ m) analytical column, a multiwavelength Waters 2487 UV-vis programmable detector operating at 240 nm, and a Breeze chromatography workstation were used. Acetonitrile plus water (40 + 60 by volume) previously brought to pH 2.7 with phosphoric acid, at a flow rate of 0.5 mL min⁻¹, was the eluant. Under the chromatographic conditions described previously the retention times were 27.6, 12.3, 8.4, 7.2, 5.7, 4.9, and 4.3 min for the compounds AZS, AZS-OH, MPS, DPA, acetic acid, malonic acid, and oxalic acid, respectively. The photodegradation product AZS-OH ([M + H]⁺ *m/e* 441) was identified by liquid chromatography-mass spectrometry analysis (LC-MS; **Figure 3**).

The concentration of AZS was calculated by using a calibration curve obtained from HPLC measurements of AZS at five different concentrations. The calibration curve, based on the average peak areas of the external standard, was linear in the range of 2–10 μ M ($r^2 = 0.992$). The detection limit for AZS was 0.1 mg L⁻¹, as calculated from the concentration of the herbicide needed to obtain a detector response approximately twice the background signal.

Isolation and Identification of Direct Photolysis Photoproducts at $\lambda = 254$ nm. A photolysis reaction was carried out to isolate photodegradation products. AZS (250 mg) dissolved in 75 mL of acetonitrile and 25 mL of water was irradiated at 254 nm for 24 h. The crude reaction mixture was concentrated by evaporation of acetonitrile under vacuum at room temperature. Unreacted AZS precipitated off and was filtered. The mother solution, left in the dark for 3 days at room temperature, yielded white crystals, which were filtered, washed three times with cold water, and dried in a desiccator. The compound was identified as the cyclic compound ADTA (**Scheme 1**). The spectral features for ADTA are as follows: IR (KBr), ν (cm⁻¹) 3470, 3357, 1687, 1629, 1584, 1545, 1368, 1193; ¹H NMR (CD₃CN), δ 7.97 (1H, s), 7.33 (1H, m), 7.0 (1H, m), 5.69 (1H, s), 4.12 (3H, s), 3.95 (3H, s), 3.65 (3H, s), 3.37 (3H, s). The remaining aqueous solution was extracted three times with diethyl ether. The combined extracts were dried over anhydrous sodium sulfate and concentrated under vacuum. The residue was separated by liquid chromatography (LC) on a 60 \times 1 cm i.d. glass column of silica gel (70–230 mesh, Merck) using light petroleum distillate (bp 40–60 °C) plus ethyl acetate (3 + 4 by volume). Volumes of 25 mL were collected, and for each aliquot thin layer chromatography (TLC) analysis was performed on Merck silica gel F₂₅₄ plates. Fractions showing similar chromatographic features were grouped and evaporated to dryness. Two products were isolated: the amine DPA and the amide 4,6-(dimethoxy)pyrimidin-2-ylurea (DPU; **Scheme 1**). DPU was obtained as white crystals: IR (KBr), ν (cm⁻¹) 3357, 3198, 1698, 1606, 1576, 1370, 1342, 1221, 1114; ¹H NMR (CD₃CN), δ 8.48 (1H, m), 7.71 (2H, m), 5.78 (1H, s), 4.89 (6H, s).

Infrared Analyses. Fourier transform infrared (FT-IR) spectra were recorded at room temperature in the range of 4000–600 cm⁻¹ using a

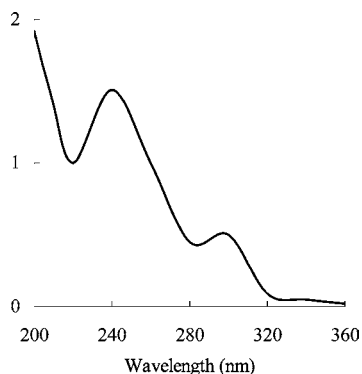
Scheme 1. Proposed Photodegradation Pathways for AZS

FT-IR Nicolet 205 spectrophotometer. The spectra are the means of at least 64 scans at 4 cm^{-1} resolution, which gives a reasonably good signal-to-noise ratio.

Nuclear Magnetic Resonance (NMR) Analyses. NMR spectra were obtained on a Bruker AC-P (300 MHz) spectrometer (Cambridge, MA) using tetramethylsilane (TMS) as an internal standard.

LC-MS Analyses. Mass spectra were performed using an Agilent G 1946 (MSD 1100) single-stage quadrupole instrument equipped with an electrospray atmospheric pressure ionization (ES-API) source. The following ES-API conditions were applied: drying gas (nitrogen) heated at $350\text{ }^\circ\text{C}$ at a flow rate of 10 L/min; nebulizer gas (nitrogen) at a pressure of 50 psi; capillary voltage in positive mode at 4000 V; fragmentor voltage at 80 V; dwell time was 460 ms.

X-ray Analyses. X-ray diffraction analysis was carried out on a Siemens SMART CCD system. Crystallographic data for ADTA are as follows: $\text{C}_{12}\text{H}_{16}\text{N}_3\text{O}_6\text{S}$; orthorhombic P n a 2₁; $a = 10.468(6)$, $b = 11.706(9)$, $c = 13.936(10)\text{ \AA}$; $V = 1707.7\text{ \AA}^3$; $M = 400.37$; $Z = 4$; $D = 1.519\text{ g cm}^{-3}$.

**Figure 2.** AZS UV spectrum.

RESULTS AND DISCUSSION

Direct Photolysis. Degradation curves for AZS at the two wavelengths tested are reported in **Figure 4**, and the related kinetic parameters are listed in **Table 2**.

The linearity of the plot of the concentration of AZS (ln values) versus time suggests that the photolysis follows pseudo-first-order kinetics. The concentration ($8\text{ }\mu\text{M}$) used in the experiments is higher than the theoretical one in rice paddy fields after an application. Actually, the amounts of pesticide in the field are often greater than those expected because of repeated applications, concentration phenomena, point pollution, etc. Therefore, the concentration chosen is the result of a settlement between instrumental and environmental considerations. The rate of disappearance in UV light was much higher than that in simulated sunlight because of the lower absorptivity of the herbicide at longer wavelengths. With UV light, AZS was converted into three products, ADTA, DPU, and DPA. The main photoproduct, ADTA (**Scheme 1**), accounted for about 70% of converted herbicide.

Suitable amounts of ADTA were obtained from UV photolysis of AZS as described under Materials and Methods. Because the spectroscopic data did not allow an unambiguous identification, the structure of the molecule was determined by single-crystal X-ray diffraction. A view of the molecule is presented in **Figure 5**.

The minor products DPA and DPU were isolated by column chromatography. DPA was identified by comparison of its chromatographic and spectroscopic features with those of an authentic sample, whereas the DPU structure was assigned by spectroscopic data (see Materials and Methods).

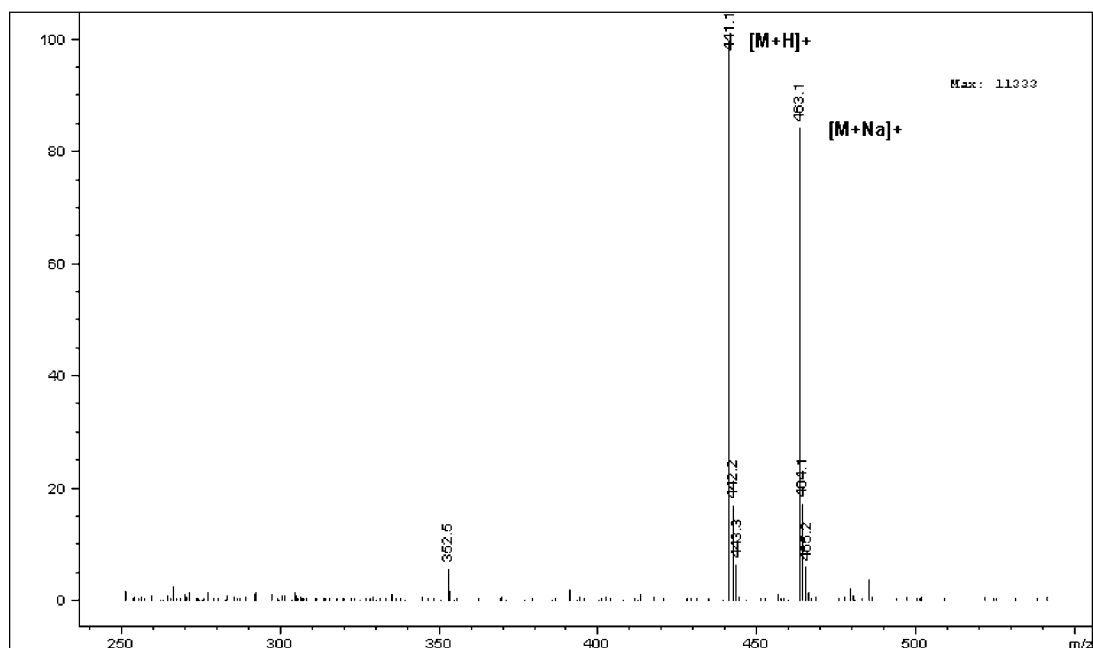


Figure 3. LC-MS spectrum of AZS-OH.

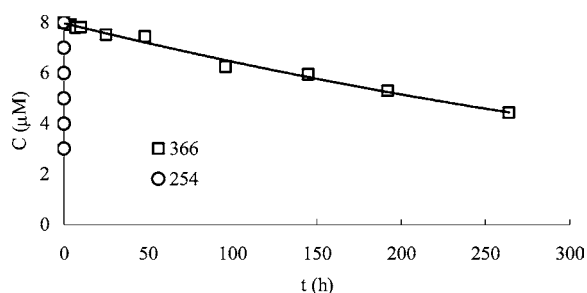


Figure 4. Degradation of AZS at 254 and 366 nm.

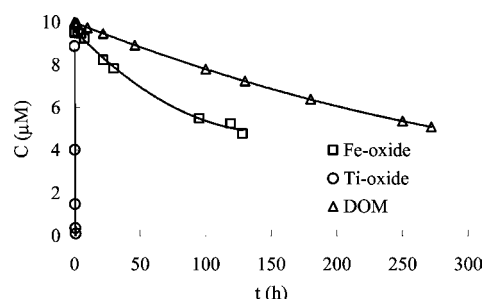


Figure 6. Indirect photodegradation of AZS.

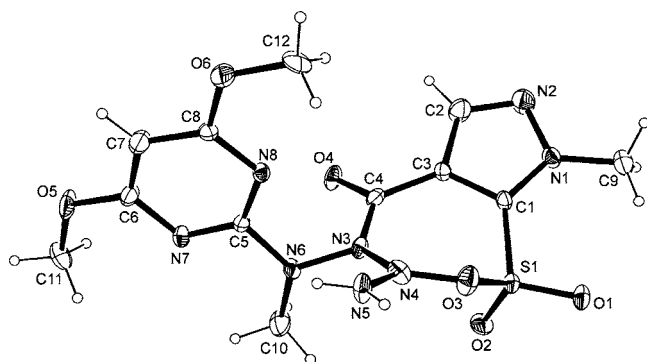


Figure 5. Atomic numbering and molecular structure of ADTA.

Table 2. Rate Constants (k) and Half-Life ($t_{1/2}$) Values for Direct Aqueous AZS Photodegradation

irradiation	k (h^{-1})	$t_{1/2}$ (h)	r
dark	4.1×10^{-4}	1680	0.997
UV	34.6	0.02	0.997
simulated sunlight	2.4×10^{-3}	286	0.993

Generally, sulfonylurea photolysis occurs through the cleavage of C–S, S–N, or N–CO bonds (3, 10). The identification of DPU and ADTA indicates that the most effective pathway in UV transformation of AZS involves the cleavage of S–N bonds.

Although it is unlikely that ADTA, DPA, and DPU, produced by UV light, occur in the environment, we cannot exclude that

Table 3. Rate Constants (k) and Half-Life ($t_{1/2}$) Values for Indirect Aqueous AZS Photodegradation under Simulated Sunlight

system	k (h^{-1})	$t_{1/2}$ (h)	r
AZS	2.4×10^{-3}	286	0.993
AZS + DOM	2.5×10^{-3}	272	0.966
AZS + Fe_2O_3	5.4×10^{-3}	128	0.994
AZS + Fe_2O_3 + ROH	4.7×10^{-3}	147	0.990
AZS + TiO_2	4.2	0.2	0.992
AZS + TiO_2 + ROH	0.5	1.5	0.941

their formation can be promoted by a suitable sensitizer. Furthermore, we thought it interesting to describe a new molecule such as ADTA, and for this purpose Supporting Information is available.

Under simulated sunlight conditions the herbicide degraded slowly, but much faster than in the dark (Table 2). In both the cases, two conversion products, 1-methyl-4-(2-methyl-2H-tetrazole-5-yl)-1H-pyrazole-5-sulfonamide (MPS; 11) and DPA, were the only byproducts observed. These products arose from the photohydrolytic cleavage of the sulfonylurea bridge.

Indirect Photolysis. The degradation curves for AZS photolysis in the presence of different colloids are reported in Figure 6, and the related kinetic parameters are listed in Table 3.

In natural water DOM plays an important role in pesticide photodegradation. As one of the primary light-adsorbing species, DOM can either promote (12) the photodegradation of organic micropollutants acting as photosensitizers or reduce (13, 14) the photolysis rate by both quenching the excited states of

organic molecules and shielding them from incident radiation. In our case the addition of DOM did not modify significantly the photodegradation rate of AZS (Table 3).

On the other hand, the addition of Fe₂O₃ to AZS solution accelerated more than twice the reaction rate, affording two major products, DPA and MPS, together with minor amounts of AZS-OH (about 5%). The presence of the hydroxylated AZS-OH compound suggests the involvement of hydroxyl radicals. To confirm this, traces of 2-propanol, an efficient trapping agent for hydroxyl radicals, were added to the suspension. The presence of the alcohol did not affect significantly the degradation rate. However, no detectable amounts of AZS-OH were observed. This suggests that in the presence of Fe₂O₃ the mechanism involving hydroxyl radicals affects the reaction rate to only a limited extent. A previous study of ours demonstrated that the AZS sulfonylurea group, acting as a bidentate ligand, chelates the ferric ion of Fe₂O₃, giving rise to a six-membered ring (11). In the dark, this interaction favored the hydrolysis of a sulfonylureic bridge with a $t_{1/2}$ of 204 h (11). Therefore, the greater rate of degradation observed in the light may be the result of hydrolysis, photohydrolysis, and, to a minor extent, photohydroxylation processes, all promoted by Fe₂O₃.

The greatest degradation rate was observed in the presence of TiO₂ ($t_{1/2}$ = 0.2 h, Table 3). After 15 min of irradiation, only the photohydroxylation product AZS-OH was present in the reaction mixture. With elapsing time, the amount of AZS-OH decreased and two new compounds, malonic and acetic acid, respectively, formed. After 22 h, the only compound present in the crude reaction mixture was oxalic acid (Scheme 1). The addition of isopropanol to the colloidal suspension decreased significantly the AZS degradation rate. This finding supports the role of hydroxyl radicals in the degradation of the herbicide and agrees with the results of Armbrust and Reilly (15).

Conclusions. UV light degraded the herbicide AZS very quickly, affording a major photoproduct arising from a photo-rearrangement pathway. In the simulated sunlight, AZS degradation was slow, and the presence of DOM did not influence the reaction rate. Instead, the photodegradation was faster in the presence of iron oxide, because of the coordination of the herbicide to iron. The resulting complexation facilitated both the hydrolytic and photolytic cleavages of the AZS C–N sulfonamidic bond. Finally, the herbicide was degraded rapidly under irradiation with TiO₂. The results indicate that light and natural colloids do not play a major role in the AZS disappearance. Therefore, the AZS photodegradation is an important method of detoxification only in the presence of an efficient photocatalyst such as titanium oxide, which affords harmless environmental photodegradation products. On the other hand, the UV light is very effective for AZS degradation, but it leads to a product of which the environmental danger is still not well-known.

Supporting Information Available: Crystal data and structure refinement, atomic coordinates, and equivalent isotropic

displacement parameters, and bond distances and angles for ADTA molecule.

LITERATURE CITED

- (1) Marquez, T.; Joshi, M. M.; Pappas Fader, T.; Massasso, W. Azimsulfuron (DPX-A8947)—a new sulfonylurea for post-emergence control of *Echinochloa* species, broadleaf and sedge weeds for southern European rice production. *Proc. Br. Crop Prot. Conf.—Weeds* **1995**, *1*, 55–62.
- (2) Barefoot, A. C.; Armbrust, K.; Fader, T.; Kato, Y.; Sato, K. Processes affecting the degradation of azimsulfuron in rice paddies. *Proc. 10th Symp. Pestic. Chem.* **1996**, 97–104.
- (3) Caselli, M. Light-induced degradation of metsulfuron-methyl in water. *Chemosphere* **2005**, *59*, 1137–1143.
- (4) Caselli, M.; Ponterini, G.; Vignali, M. Irradiation-wavelength dependent photochemistry of the bichromophoric sulfonylurea chlorsulfuron. *J. Photochem. Photobiol. A* **2001**, *138*, 129–137.
- (5) Pusino, A.; Braschi, I.; Petretto, S.; Gessa, C. Photodegradation of herbicide triasulfuron. *Pestic. Sci.* **1999**, *55*, 479–481.
- (6) Vuillet, E.; Emmelin, C.; Chovelon, J. M.; Guillardand, C.; Herrmann, J. M. Photocatalytic degradation of sulfonylurea herbicides in aqueous TiO₂. *Appl. Catal. B: Environ.* **2002**, *38*, 127–137.
- (7) Vuillet, E.; Chovelon, J. M.; Guillard, C.; Herrmann, J. M. Factors influencing the photocatalytic degradation of sulfonylurea herbicides by TiO₂ aqueous suspension. *J. Photochem. Photobiol. A* **2003**, *159*, 71–79.
- (8) European Commission Directive 94/37/EC of 22 July 1994 concerning the placing of pesticides on the market.
- (9) Landa, E. R.; Gast, R. G. Evaluation of crystallinity in hydrated ferric oxides. *Clays Clay Min.* **1973**, *21*, 121–130.
- (10) Weiss, B.; Dürr, H.; Haas, H. J. Photochemistry of sulfonamides and sulfonylureas: a contribution to the problem of light-induced dermatoses. *Angew. Chem., Int. Ed. Engl.* **1980**, *19*, 648–650.
- (11) Pinna, M. V.; Pusino, A.; Gessa, C. Sorption and degradation of azimsulfuron on iron(III)-rich soil colloids. *J. Agric. Food Chem.* **2004**, *52*, 8081–8085.
- (12) Richard, C.; Vialaton, D.; Aguer, J. P.; Andreux, F. Transformation of monuron photosensitized by soil extracted humic substances: energy or hydrogen transfer mechanism? *J. Photochem. Photobiol. A* **1997**, *111*, 264–271.
- (13) Dimou, A. D.; Sakkas, V. A.; Albanis, T. A. Trifluralin photolysis in natural waters and under the presence of isolated organic matter and nitrate ions: kinetics and photoproduct analysis. *J. Photochem. Photobiol. A* **2004**, *163*, 473–480.
- (14) Dimou, A. D.; Sakkas, V. A.; Albanis, T. A. Metolachlor photodegradation study in aqueous media under natural and simulated solar irradiation. *J. Agric. Food Chem.* **2005**, *53*, 694–701.
- (15) Armbrust, K. L.; Reilly, D. Rate constants of selected pesticides with photochemically generated hydroxyl radicals. In *Proceedings of the 211th ACS National Meeting*, New Orleans; American Chemical Society: Washington, DC, 1996; p AGRO-189.

Received for review March 28, 2007. Revised manuscript received June 4, 2007. Accepted June 5, 2007. Financial support was provided by the Italian Ministry of University and Scientific and Technological Research (PRIN Project).

JF070897K